SIMULATION ANALYSIS AND PARAMETER OPTIMIZATION OF A TWIN-ROLL SOIL-CRUSHING DEVICE FOR A POTATO HARVESTER

马铃薯收获机对辊式碎土装置仿真分析与参数优化

Yangbiao HUANG[1)], Song CHEN[1)], Zihao OU[1)], Qingmiao XIANG[1)], Bei WU*[1,2)], Bang JI[1,2)], Zhichao FANG[1,2)], Fangping XIE[1,2)]

[1)] Hunan Agricultural University, College of Mechanical and Electrical Engineering, Changsha / China;

[2)] Hunan Key Laboratory of Intelligent Agricultural Machinery and Equipment, Changsha / China

Tel: +86 15802521582; E-mail: wubei@hunau.edu.cn

Corresponding author: Bei Wu

DOI: https://doi.org/10.35633/inmateh-79-74

Keywords: *Potato harvester; Roller-type Soil Crushing Device; Potato-soil separation device; EDEM; Heavy clay soil*

ABSTRACT

Winter potato cultivation in paddy fields in southern China can improve land-use efficiency and increase farmers' incomes. However, compared with those in northern China, paddy soils in southern China are generally heavy, cohesive, and compacted, resulting in poor mechanized potato-harvesting performance and restricting the development of the potato industry. To improve potato-soil separation efficiency under heavy clay soil conditions, a twin-roll soil-crushing device was installed ahead of a conventional chain-and-rod potato-soil separation device based on the characteristics of clayey soils in southern China. This configuration formed a two-stage separation process involving soil crushing followed by screening. The soil-crushing process was theoretically analyzed, a discrete element model of the soil-crushing and screening device was established, and the soil-crushing and potato–soil separation processes were numerically simulated. Response surface simulation experiments were conducted using rib height, number of ribs, and twin-roll rotational speed as the experimental factors, with soil-screening efficiency and the maximum force acting on the potato tubers as the response variables. The results showed that the twin-roll soil-crushing device effectively disturbed and crushed the soil during operation. Increasing the rib height and twin-roll rotational speed enhanced the soil-disturbance and crushing effects. The optimal structural and operating parameters of the twin-roll soil-crushing device were a rib height of 30 mm, three ribs, and a twin-roll rotational speed of 323.70 r/min. A simulation verification test conducted using these optimal parameters yielded a soil-screening efficiency of 72.80% and a maximum force acting on the potato tubers of 15.45 N. Field-test results showed that the potato harvester equipped with the soil-crushing device achieved a tuber damage rate of 0.285%, a skin-damage rate of 2.38%, and a tuber loss rate of 3.18%, thereby meeting the requirements of the applicable national standards. These findings provide a reference and technical support for the development of potato-harvesting machinery suitable for heavy clay soil conditions.

摘要

中国南方水稻田冬种马铃薯能提高土地利用率，促进农民增收，相较于北方，南方水稻田土壤黏重板结，常见马铃薯机械化收获作业效果不佳，制约了产业的发展。为了提高黏重土壤下薯土分离效率，本研究针对中国南方黏土土壤特点，在传统链杆式薯土分离装置前设计了对辊式碎土装置，形成 “先破碎、后筛分” 两级分离流程，提高薯土分离效率，对碎土过程进行了理论分析，构建了碎土筛分装置离散元模型并对土壤破碎和薯土分离过程进行了数值模拟。以碎土装置的凸棱高度、凸棱数量、对辊转速为试验因素，以土壤筛分效率和薯块最大受力为评价指标，开展了响应面仿真试验，结果表明，对辊式碎土装置在工作时对土壤起到了扰动和破碎作用，增加凸棱高度和提高对辊转速能够增加碎土装置对土壤的扰动和破碎作用。对辊式碎土装置的最优结构运行参数为凸棱高度 30 mm，凸棱数量为 3 个，对辊转速 323.70 r/min，以此最优参数开展仿真验证试验，土壤筛分效率为72.80%，薯块最大受力为15.45N。田间试验结果表明，配置有碎装置的马铃薯收获机伤薯率为0.285%，破皮率为2.38%，损失率为3.18%，满足国家标准要求。研究结果能为黏重土壤条件下马铃薯收获机具的研发提供参考和支撑。

Yangbiao Hunag, Ms. Stud.; Song Chen, Ms. Stud.; Zihao Ou, Ms. Stud.; Qingmiao Xiang, Ms. Stud.; Bei Wu, Lect. Ph.D.; Bang JI, Prof. Ph.D. Zhichao Fang Lect. Ph.D. Pingfang Xie Prof. Ph.D.

INTRODUCTION

The annual potato planting area in China exceeds 6 million hectares, making the potato industry a vital pillar for promoting rural revitalization and ensuring national food security *(Li et al., 2022)*. In the southern regions, cultivating potatoes in winter-idle rice fields enhances land-use efficiency and complements the market supply season, offering broad development prospects. However, potato-growing areas in the south are predominantly located in hilly and mountainous regions characterized by heavy, compact clay soils. Furthermore, the harvest season often coincides with the rainy season, leading to high soil moisture content. These harsh conditions pose severe challenges for mechanized harvesting (*Jiang et al., 2016*). Existing harvesting machinery, primarily designed for the loose, sandy soils of the north, struggles to adapt to southern clay soils, resulting in low soil-tuber separation efficiency and a low rate of exposed tubers (*Bei et al., 2021; Li et al., 2022; Lv et al., 2017*). Therefore, designing potato harvesting machinery tailored to heavy clay soil and hilly terrain is of great significance for the southern winter potato industry (*Wang et al., 2021; Zhang et al., 2021; Zhongcai et al., 2019; Zhou et al., 2021*).

To achieve efficient, low-loss potato harvesting in heavy clay soils, existing research has primarily explored mechanical structure innovations and operational parameter optimizations. In terms of mechanical structures, various separation mechanisms have been developed. For instance, digging devices with vibration functions have been designed to reduce digging resistance in sticky soils (*Lv et al., 2015*). Multi-stage chain-and-rod screening devices and concave-bar structures have been implemented to increase soil disturbance and enhance separation efficiency (*Xiaoxuan et al., 2024; Qingmiao et al., 2024*). Additionally, roller structures with staggered rod arrangements *(Shi et al., 2012)* and flexible rotary-vibration systems *(Xiang et al., 2020)* have been developed to reduce clogging and mechanical damage. Regarding operational parameters, studies have demonstrated that matching a "high frequency and low amplitude" vibration with appropriate linear velocities can improve the soil crushing rate and minimize tuber damage (*CAAMS, 2007; Li et al., 2016; Li et al., 2021*). Furthermore, recent studies have continuously emphasized the importance of optimizing machine-soil interaction mechanisms through Discrete Element Method (DEM) simulations to improve separation and digging performance in complex agricultural terrains (*Fu et al., 2023; Ge et al., 2025*).

Despite these advancements in screening structures and kinematics, a critical research gap remains: existing separation mechanisms are primarily designed to sieve pre-loosened soil rather than actively break hard, cohesive clods. Practical experiments indicate that severe soil compaction and high viscosity are the fundamental causes of incomplete soil-tuber separation in southern fields. Under such conditions, standard chain-and-rod or vibrating separation devices lack the initial mechanical impact required to shatter the compacted clay structure. Consequently, large, wet soil clods carry the tubers over the sieves without separating, rendering the subsequent screening stages ineffective. To overcome this bottleneck, it is imperative to introduce a robust, active soil-breaking mechanism prior to the main screening device to destroy the compacted soil structure at the earliest stage.

To address this gap, a twin-roll soil-crushing device was installed ahead of a conventional chain-and-rod separation conveyor. The protruding ribs on the rolls exert impact and shear forces on compacted clay clods, thereby promoting their fragmentation. Based on a theoretical kinematic analysis, a discrete element model of the soil-crushing and screening device was established to simulate the potato–soil separation process. A response surface methodology (RSM) simulation experiment was conducted using rib height, number of ribs, and twin-roll rotational speed as the experimental factors, with soil-screening efficiency and the maximum force acting on the potato tubers as the response variables. This study aimed to optimize the structural and operating parameters of the twin-roll soil-crushing device and provide a theoretical basis and technical reference for the development of efficient potato-harvesting machinery suitable for heavy clay soils.

MATERIALS AND METHODS

Structure of the twin-roll soil crushing device

The potato harvester equipped with a twin-roll soil-crushing device was designed for operation in the heavy clay soils of southern China. As shown in Fig. 1, the machine mainly comprises a digging shovel, disc coulters, a transmission system, a lateral conveying device, a debris-removal device, a potato–soil separation device, and a soil-crushing device. According to the *Agricultural Machinery Design Manual* (CAAMS, 2007), the potato–soil separation device was designed with a length of 1.75 m, and the chain-and-rod conveyor was inclined at an angle of 30° to the horizontal *(Ma et al., 2012; Zhou et al., 2021)*.

To facilitate the fragmentation of heavy, cohesive soil and improve the screening efficiency of the potato–soil separation device, the twin-roll soil-crushing device was installed between the digging shovel and the potato–soil separation device. The device consists of two rolls rotating in the same direction, with three to five protruding ribs arranged on the surface of each roll. During operation, the twin-roll soil-crushing device rotates rearward and conveys the potato–soil mixture toward the separation device. Simultaneously, the protruding ribs exert bending forces on the soil clods, causing them to fracture.

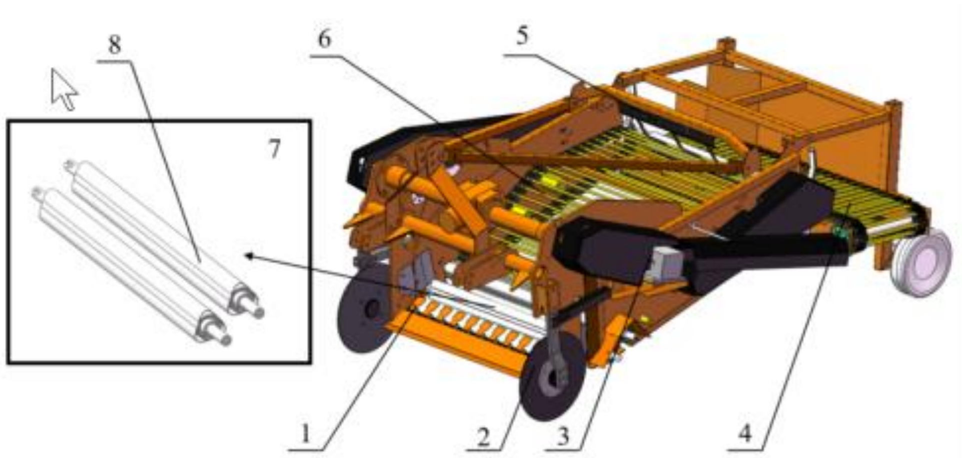

Fig. 1 - Structural schematic of the potato harvester and twin-roll soil-crushing device

1. Digging shovel; 2. Disc coulter; 3. Transmission system; 4. Lateral conveying device; 5. Debris removal device; 6. Potato-soil separation device; 7. Twin-roll soil-crushing device; 8. Protruding rib

Development of the Simulation Model

Development of the Potato Tuber and Soil Models

During potato-harvester operation, the interactions among the potato tubers, soil, and soil-crushing device are highly complex. Soil clods undergo fragmentation under external excitation, whereas the crushing rolls can be regarded as rigid bodies. EDEM software was used to simulate the interactions among the potato tubers, soil, and soil-crushing device and thereby evaluate the performance of the device.

The particle model of the potato tuber is shown in Fig. 3. A multisphere clump model was used to represent the potato tuber *(Qingmiao et al., 2024)*, with its three principal dimensions set to 62 mm × 52 mm × 52 mm. The Hertz–Mindlin (no slip) contact model was applied to tuber-tuber, tuber-soil, and tuber-machine interactions. The soil particles were modeled as spheres with a radius of 3 mm. Considering the characteristics of heavy clay soils in southern China *(Bei et al., 2021; Ren et al., 2017)*, the Hertz–Mindlin with Bonding V2 contact model was used to simulate interparticle bonding within the soil. Based on the moisture-content range of heavy clay soils in southern China, the contact radius of the soil particles was set to 3.75 mm. The simulation parameters of the potato tubers and soil particles are presented in Table 1 *(Qingmiao et al., 2024; Xie et al., 2020)*. Some parameters for the soil-particle and metal-component models were obtained from the literature *(Minzhang et al., 2024; Linrong et al., 2018; Wei et al., 2019; Zhongcai et al., 2020)*, whereas the remaining parameters, including those of the potato-tuber model, were determined experimentally.

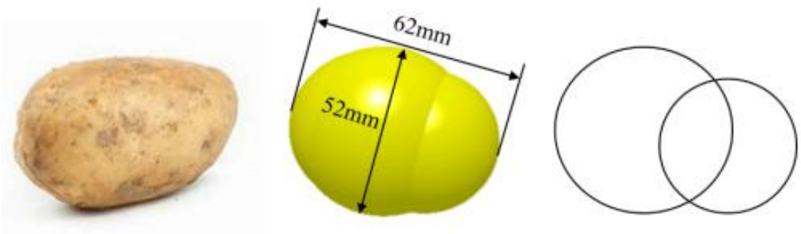

Fig. 2 - Multisphere particle model of a potato tuber

Table 1

Parameters of the Discrete Element Model

Parameter	Numerical value	Parameter	Numerical value
Poisson's ratio of potato tubers	0.5	Coefficient of static friction between potato tubers and rods	0.4
Shear modulus of potato tubers / MPa	1.366	Coefficient of rolling friction between potato tubers and rods	0.1
Potato-tuber density / (kg·m^{-3})	1100	Normal stiffness between soil particles / (N·m^{-1})	1.4 × 10^{6}
Coefficient of restitution between potato tubers	0.79	Maximum normal stress between soil particles / MPa	0.235
Coefficient of static friction between potato tubers	0.5	Tangential stiffness between soil particles / (N·m^{-1})	1 × 10^{6}
Coefficient of rolling friction between potato tubers	0.024	Poisson's ratio of the rod material	0. 3
Poisson's ratio of soil	0.38	Shear modulus of the rod material / MPa	3. 1 × 10^{5}
Shear modulus of soil / MPa	1	Density of the rod material / (kg·m^{-3})	7 800
Soil-particle density / (kg·m^{-3})	2670	Coefficient of restitution between soil particles and rods	0.16
Coefficient of restitution between soil particles	0.37	Coefficient of static friction between soil particles and rods	0.6
Coefficient of static friction between soil particles	0.6	Coefficient of rolling friction between soil particles and rods	0.35
Coefficient of rolling friction between soil particles	0.26	Coefficient of restitution between potato tubers and rods	0.5
Coefficient of restitution between potato tubers and soil particles	0.06	Coefficient of static friction between potato tubers and soil particles	0.5

Development of the Simulation Model of the Soil-Crushing and Screening Device

The geometric model of the soil-crushing and screening device is shown in Fig. 4. A particle factory measuring 1,100 mm × 1,000 mm × 600 mm was established at the front of the model to generate soil and potato-tuber particles. Below the particle factory, a conveyor belt was created using the moving-plane tool in EDEM to convey the potato–soil mixture rearward. The conveyor-belt speed was set to 1 m/s, corresponding to the forward speed of the potato harvester. A soil-compaction plate was positioned above the conveyor belt to compact the potato–soil mixture before it entered the harvesting components, thereby simulating compacted clay soil. The machine model consisted of a digging shovel, a twin-roll soil-crushing device, and a chain-and-rod potato–soil separation device, all of which were modeled as steel components. The rolls of the soil-crushing device were set to rotate rearward. The chain-and-rod separation device comprised 69 rods, each of which was assigned linear and circular motion cycles. A fixed time interval was applied between the motions of adjacent rods to simulate the continuous operation of the chain-and-rod device. In the model, the rod diameter was 11 mm *(Sun et al., 2019)*, the linear speed was 1.7 m/s, and the center-to-center spacing between adjacent rods was 50 mm. Accordingly, the time interval between the motions of adjacent rods was calculated to be 0.02941 s. Based on the dimensions and linear speed of the chain-and-rod separation device, the angular velocity of the rods in the circular-motion section was calculated to be 20.98765 rad/s, and the time required for one complete circulation was 2.64706 s. At the position of the shaking device, a sinusoidal translational motion perpendicular to the screening surface was applied to each rod at a frequency of 5 Hz to simulate the vibrational action of the device. A potato-and-soil collection bin was positioned behind the separation device to collect and quantify the residual soil and potato tubers discharged from the screening surface, thereby allowing the potato–soil separation performance to be evaluated.

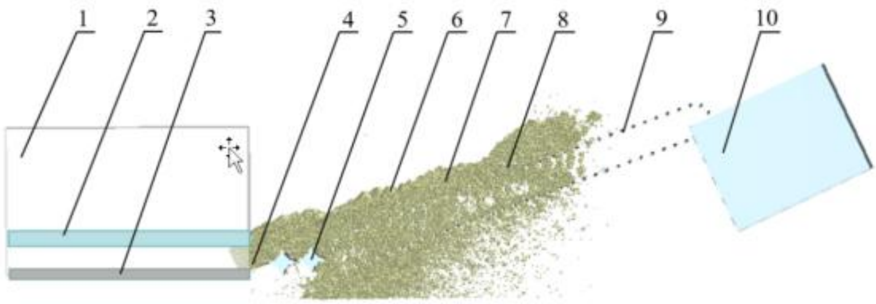

Fig. 3 - Simulation model of the potato–soil separation device

1. Particle Factory; 2. Soil Compaction Plate; 3. Conveyor Belt; 4. Digging Shovel; 5. Twin-roll soil-crushing device; 6. Potato Tuber Particles; 7. Soil Particles; 8. Shaking Device; 9. Chain-and-rod separation device; 10. Potato-and-soil collection bin

Simulation Process and Parameter Settings

Before the simulation, a mixture of soil and potato-tuber particles was generated. A total of 600,000 soil particles forming the lower soil layer were generated between 0 and 0.8 s. The generation of 20 potato-tuber particles began at 0.5 s. Subsequently, 1,300,000 soil particles forming the upper soil layer were generated over a period of 0.4 s, beginning at 0.8 s. After all particles had been generated, the soil-compaction plate moved downward to compact the soil, forming a 180-mm-thick soil–potato–soil layered mixture. The conveyor belt was activated at 1.6 s and transported the potato–soil mixture rearward into the twin-roll soil-crushing device and the chain-and-rod potato–soil separation device. The total simulation duration was 6 s. The simulation time step was set to 20% of the Rayleigh time step, which was 1.037×10^{-4} s, and the data-saving interval was set to 0.1 s.

Simulation Test Method

Experimental Design

During operation, the structural and operating parameters of the twin-roll soil-crushing device affect both soil-screening efficiency and the likelihood of potato-tuber damage. To determine the optimal parameters of the soil-crushing device, a three-factor, three-level Box–Behnken response surface design was developed using Design-Expert software. Rib height h, number of ribs q, and twin-roll rotational speed n were selected as the experimental factors. The factor levels are presented in Table 2, and the experimental design is presented in Table 3. Simulation tests were then performed using the model described above, and the resulting data were used to optimize the parameters of the twin-roll soil-crushing device.

Table 2

Experimental factors and levels

Level	Factor		
	Rib height *h* / mm	Number of ribs *q* / pieces	Twin-roll rotational speed *n* / (r/min)
1	20	3	200
2	25	4	300
3	30	5	400

Measurement of Response Variables

Soil-screening efficiency *E* and the mean maximum force acting on the potato tubers *E* were selected as the response variables in the response surface experiment. Soil-screening efficiency was used to evaluate the combined soil-crushing and screening performance of the twin-roll soil-crushing device and the chain-and-rod separation device. In each simulation test, EDEM was used to determine the mass of residual soil collected in the potato-and-soil collection bin and the total mass of soil generated. Soil-screening efficiency was calculated as follows *(Sun et al., 2019)*:

$$E=1-\frac{M_r}{M_t}\times100\% \quad (1)$$

where, *E* is the soil-screening efficiency M_r is the mass of residual soil collected in the potato-and-soil collection bin, [kg]; M_t is the total mass of soil generated, [kg].

The force acting on the potato tubers was used as an indicator of their risk of mechanical damage during conveying and screening. EDEM was used to determine the maximum force experienced by each of the 20 potato tubers during each simulation test. The mean of these individual maximum values was then calculated and used as the force response variable.

RESULTS

Analysis of Soil Disturbance

The motion of the potato–soil mixture above the twin-roll soil-crushing device was visualized using the EDEM post-processing module. The soil particles were color-coded according to their velocity. Particles approaching red had higher velocities, indicating greater soil disturbance, whereas particles approaching blue-green had lower velocities and were subjected to less disturbance. The soil-particle disturbance produced by the twin-roll soil-crushing device is shown in Fig. 5.

As shown in Fig. 5, a distinct red region formed among the soil particles above the twin-roll soil-crushing device, indicating that the device effectively disturbed the soil and promoted clod fragmentation. As rib height *h* and twin-roll rotational speed *n* increased, the red region expanded, indicating enhanced soil disturbance and crushing. By contrast, when the number of ribs *q* increased from three to five, no marked change in the size of the red region was observed, suggesting that the number of ribs had a limited effect on soil disturbance within the investigated range.

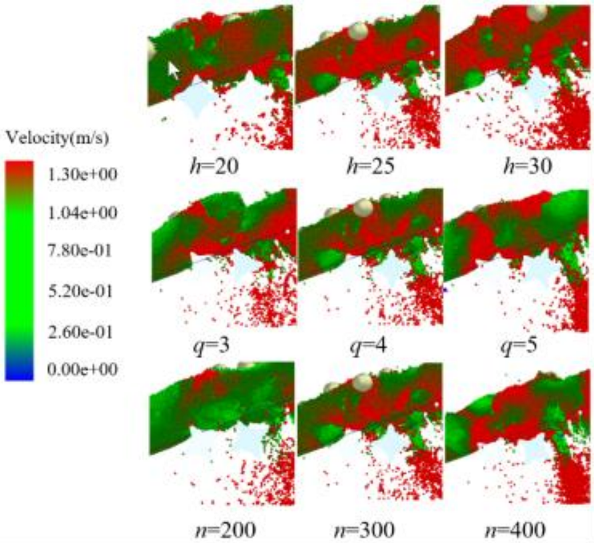

Fig. 5 - Soil-disturbance patterns under different operating conditions

Analysis of Response Surface Experiment Results

The response surface experiment results are presented in Table 3. Regression analysis and analysis of variance (ANOVA) were performed using Design-Expert software, and the results are presented in Table 4. The P-values of the regression models for soil-screening efficiency and the maximum force acting on the potato tubers were both less than 0.05, whereas the P-values of the lack-of-fit terms were greater than 0.05. Thus, both regression models were statistically significant and adequately fitted the experimental data. After removing nonsignificant terms with P-values greater than 0.10, the regression equations for soil-screening efficiency and the maximum force acting on the potato tubers were obtained, as given in Eqs. (2) and (3), respectively.

$$E = 69.14888 - 0.025552n - 12.22375q + 2.65918h + 0.003305nh + 0.344500qh - 0.000072n^2 - 0.089574h^2 \quad (2)$$

$$F = +63.94900 - 0.298455n - 24.2665q + 4.2125h - 0.0193nq + 0.00397nh + 0.000416n^2 + 4.0005q^2 - 0.11398005h^2 \quad (3)$$

Table 3

Response surface experimental design and results

Run number	Factor			Experimental result	
	Rib height *h* / mm	Number of ribs *q* / pieces	Twin-roll rotational speed *n* / (r/min)	Soil screening efficiency *E* / %	Mean maximum force acting on potato tubers *F* / N
1	200	3	25	77.38	25.27
2	400	3	25	79.13	24.48
3	200	5	25	69.78	34.58
4	400	5	25	73.11	26.07
5	200	4	20	70.98	27.81
6	400	4	20	70.64	17.66
7	200	4	30	72.29	19.87
8	400	4	30	78.56	17.66
9	300	3	20	75.68	19.28
10	300	5	20	64.6	23.85

Run number	Factor			Experimental result	
	Rib height *h* / mm	Number of ribs *q* / pieces	Twin-roll rotational speed *n* / (r/min)	Soil screening efficiency *E* / %	Mean maximum force acting on potato tubers *F* / N
11	300	3	30	78.62	19.57
12	300	5	30	74.43	19.68
13	300	4	25	76.15	19.46
14	300	4	25	75.41	19.77
15	300	4	25	76.67	20.74
16	300	4	25	76.01	17.79
17	300	4	25	75.9	19.46

Table 4

Analysis of variance for the response surface regression models

Source of variation	Soil screening efficiency *E* / %				Source of variation	Mean maximum force exerted on the potato mass *F* / N			
	Sum of squares	df	F-value	P-value		Sum of squares	df	F-value	P-value
model	0.0229	9	63.02	< 0.0001	**model**	314.21	9	19.35	0.0004
n	0.0015	1	37.62	0.0005	***n***	58.64	1	32.49	0.0007
q	0.0104	1	258.78	< 0.0001	***q***	30.32	1	16.80	0.0046
h	0.006	1	150.05	< 0.0001	***h***	17.46	1	9.68	0.0171
nq	0.0001	1	1.55	0.2535	***nq***	14.95	1	8.28	0.0237
nh	0.0011	1	27.17	0.0012	***nh***	15.78	1	8.75	0.0212
qh	0.0012	1	29.52	0.001	***qh***	4.96	1	2.75	0.1414
n^2	0.0002	1	5.07	0.059	n^2	72.64	1	40.25	0.0004
q^2	0.0001	1	2.44	0.1626	q^2	67.40	1	37.35	0.0005
h^2	0.0021	1	51.19	0.0002	h^2	34.15	1	18.92	0.0034
residual	0.0003	7			**residual**	12.63	7		
Lack of fit	0.0002	3	3.25	0.1424	**Lack of fit**	8.09	3	2.37	0.2113
Pure error	0.0001	4			**Pure error**	4.54	4		
Cor total	0.0231	16			**Cor total**	326.84	16		

Parameter Optimization and Validation

Based on the regression Eqs. (2) and (3), numerical parameter optimization was performed using the optimization module in Design-Expert. The objective functions and constraints were defined as follows:

$$\begin{cases} \max E(n,\ q,\ h) \\ \min F(n,\ q,\ h) \\ 20\text{mm} \le A \le 30\text{mm} \\ B \in \{3,\ 4,\ 5\} \\ 200\text{r/min} \le C \le 400\text{r/min} \end{cases} \tag{4}$$

The optimal structural and operating parameters of the twin-roll soil-crushing device were a rib height h of 30.00 mm, three ribs (q =3), and a twin-roll rotational speed n of 323.70 r/min. The simulation model was configured using this optimal parameter combination, and a verification simulation was subsequently conducted. The resulting soil-screening efficiency was 72.80%, and the mean maximum force acting on the potato tubers was 15.45 N.

Verification Test

Based on the optimal structural and operating parameters determined above, a prototype of the twin-roll soil-crushing device was manufactured and installed on a 4U-1100 side-discharging potato harvester. Field tests were subsequently conducted in a paddy field in Liuyang City, Hunan Province, China. The potatoes, cultivar Xingjia No. 2, were grown using ridge cultivation, and the soil moisture content at the time of testing was 16.3%. The ridge height, ridge-top width, ridge-base width, and furrow width were 300, 700, 1,100, and 400 mm, respectively. The field-test conditions are shown in Fig. 6, and the results are presented in Table 5. The tuber damage rate, skin-damage rate, and tuber loss rate of the potato harvester equipped with the twin-roll soil-crushing device satisfied the requirements of the agricultural industry standard NY/T 648-2015 *(MOA, 2015)*.

Fig. 6 - Field verification test

Table 5

Test Results of Field Experiment

Evaluation criterion	Tuber damage rate/%	Skin-damage rate/%	Tuber loss rate/%
Government standard	≤2	≤3	≤4
Measured value	0.285	2.38	3.18

CONCLUSIONS

To improve potato–soil separation under heavy clay soil conditions, a twin-roll soil-crushing device was installed ahead of a conventional chain-and-rod potato–soil separation device. The soil-crushing process was theoretically analyzed, a discrete element model of the soil-crushing and potato–soil separation system was developed, and the corresponding processes were simulated. The main conclusions are as follows:

(1) The twin-roll soil-crushing device effectively disturbed the soil and promoted clod fragmentation during operation. Increasing the rib height and twin-roll rotational speed enhanced the soil-disturbance and crushing effects. By contrast, the number of ribs had no marked effect on the observed soil-disturbance pattern within the investigated range.

(2) The response surface simulation results indicated that the optimal structural and operating parameters of the twin-roll soil-crushing device were a rib height of 30 mm, three ribs, and a twin-roll rotational speed of 323.70 r/min. A verification simulation conducted using this optimal parameter combination yielded a soil-screening efficiency of 72.80% and a mean maximum force of 15.45 N acting on the potato tubers.

(3) Field-test results showed that the potato harvester equipped with the twin-roll soil-crushing device achieved a tuber damage rate of 0.285%, a skin-damage rate of 2.38%, and a tuber loss rate of 3.18%. All three performance indicators satisfied the requirements of the national standards.

ACKNOWLEDGEMENT

This research was supported by the Hunan Provincial Natural Science Foundation of China (2024JJ5194) and the Hunan Agriculture Research System (HARS-02).

REFERENCES

[1] Bei W. Tianci H., Xuanxuan Q., Tianlin Z., Xiushan W., Fangping X., (2021), Design and experimental study of potato-soil separation device for sticky soils condition. *Applied Sciences*, vol. 11, no. 22, pp. 10959. Basel / Switzerland.

[2] Chinese Academy of Agricultural Mechanization Sciences (CAAMS). (2007). *Design Handbook of Agricultural Machinery* (农业机械设计手册), vol.1, China Agricultural Science and Technology Press, pp.1086-1088. ISBN: 9787802333352. Beijing / China.

[3] Fu Y., Ren S., Tang P., Leng Y., Chen X., Tu X., Lv X., (2023). Design and simulation test of digging device for small potato harvester. *INMATEH-Agricultural Engineering*, vol. 69, no. 1. Bucharest/Romania.

[4] Ge J., Zhu X., Cao C., Fang L., Sun Y., Lu J., Qin K., (2025). Experimental and DEM-based analysis of lateral stress and soil particle displacement under the action of a subsoiler. *INMATEH-Agricultural Engineering*, vol. 76, no. 2, pp. 862-871. Bucharest / Romania.

[5] Jiang L., Ma X., Wu T., Chen X., Sun G., Tan Y., Lu F., Chen G., (2016). Application status and research prospect of southern winter planting potato harvesting machine(南方冬种马铃薯收获机的应用现状与研究展望), *Journal of Agricultural Mechanization Research*, vol.38, no.07, pp. 263-268. Heilongjiang/China.

[6] Li Z., Jiang J., Zhan C., Yue Q., Sui X., (2016). Design and experimental study on the conveying chain soil cleaning device of potato harvester (薯类收获机输送链条清土装置的设计和试验研究). *Journal of Agricultural Mechanization Research*, vol. 38, no. 02, pp. 123-127. Heilongjiang/China.

[7] Li Y., Zhang Z., Wang Y., Wang H., Pang Y., Zhang Z., (2021). Design and experiment of multistage conveying and separating device for potato harvester (马铃薯收获机多级输送分离装置设计与试验). *Journal of Shenyang Agricultural University*, vol.52, no.06, pp.758-768. Shenyang/China.

[8] Li J., Lü Y., Sun Y., Lin Y., (2022). Design and experiment of separating and lifting device of potato harvester based on equivalent radius method (马铃薯收获机分离升运装置设计与试验—基于当量半径法), *Journal of Agricultural Mechanization Research*, vol.44, no.12, pp. 199-206+256. Heilongjiang/China.

[9] Wei X., Mingliang W., Jiangnan L., Wei Q., Lan M., Jiajie L., (2019). Calibration of simulation physical parameters of clay loam based on soil accumulation test (基于堆积试验的黏壤土仿真物理参数标定), *Transactions of the Chinese Society of Agricultural Engineering*, vol.35, no.12, pp.116-123, Beijing/China.

[10] Lv J., Tian Z., Wu J., Yang Y., Shang Q., Wang Y., Liu Z., (2015). Design and experiment of 4U1Z vibrating potato digger (4U1Z 型振动式马铃薯挖掘机的设计与试验). *Transactions of the Chinese Society of Agricultural Engineering*, vol. 31, no. 12, pp.39-47. Beijing/China.

[11] Lv J., Sun H., Dui H., Peng M., Yu J., (2017). Design and experiment on conveyor separation device of potato digger under heavy soil condition (粘重土壤下马铃薯挖掘机分离输送装置改进设计与试验). *Transactions of the Chinese Society for Agricultural Machinery*, vol. 48, no. 11, pp. 146-155. Beijing/China.

[12] Ma L., Chu X., Zhang L., Yan Z., Wu H., He S., (2012). Modal analysis of potato separating device based on ANSYS workbench (马铃薯土薯分离装置模态分析—基于 ANSYS Workbench). *Journal of Agricultural Mechanization Research*, vol. 34, no. 10, pp. 62-65. Heilongjiang/China.

[13] Ministry of Agriculture of the People's Republic of China (MOA), (2015). *Technical specification of quality evaluation for potato harvesters NY/T 648-2015* (马铃薯收获机质量评价技术规范: NY/T648-2015), Standards Press of China, Beijing/China.

[14] Minzhang L., Fangping X., Dawei L., Xiushan W., (2024). Analysis and experiment of the power of blade roller in reverse-rotary ditching machine based on the granular scale effect (基于颗粒放尺效应的逆旋开沟机刀辊功耗分析与试验), *Transactions of the Chinese Society of Agricultural Engineering*, vol.40, no.7, pp.83-92, Beijing/China.

[15] Qingmiao X., Bei W., Fangping X., Zhichao F., Huaiyuan Q., Zhuo L., (2024). Simulation analysis and optimization of concave bar potato-soil separation device. *INMATEH-Agricultural Engineering*, vol. 74, no. 3, pp. 460-472. Bucharest/Romania.

[16] Ren J., (2017). *Research on the mechanism of subsoiling in paddy soil using DEM* (*基于离散元法的水稻土深松耕作机理研究*). MSc Thesis, Nanjing Agricultural University, Nanjing/China.

[17] Shi, L., Wu, J., Zhao, W., Sun, W., Wang, D., Li, H., Liu, Q., (2012). Development and experiment of disc-grid type potato digger (圆盘栅式马铃薯挖掘机的研制与试验). *Transactions of the Chinese Society of Agricultural Engineering*, vol. 28, no. 24, pp. 15-21. Beijing/China.

[18] Sun H., (2019). *Design and experimental research on transporting and separating device of lifting chain potato digger (升运链式马铃薯挖掘机输送分离装置的设计与试验研究)*. MSc Thesis, Northeast Agricultural University, Haerbin/China.

[19] Wang H., (2021) . *Mountain self-propelled potato combine harvester design and experiment (山地自走式马铃薯联合收获机设计与试验)*. MSc Thesis, Kunming University of Science and Technology, Kunming /China.

[20] Linrong S., Wei S., Wuyun Z., Xiaoping Y., Bin F., (2018). Parameter determination and validation of discrete element model of seed potato mechanical seeding (马铃薯种薯机械排种离散元仿真模型参数确定及验证), Transactions of the Chinese Society of Agricultural Engineering, vol.34, no.6, pp.35-42, Beijing/China.

[21] Xiang J., (2020). *Research and experiment of clay potato separation device for potato harvester (适用于粘土的马铃薯收获机土薯分离装置的设计与试验)*. MSc Thesis, Sichuan Agricultural University, Yaan/China.

[22] Xiaoxuan, Z., Jin L., Chenglin Z., Yueyun Z., Xinwu D., (2024). Design and experimentation of small potato harvester for heavy soil in hilly and mountainous areas. *Agronomy*, vol.14, no.9, pp. 2131. Basel/ Switzerland.

[23] Xie F., Wu Z., Wang X., Liu D., Wu B., Zhang Z., (2020). Calibration of discrete element parameters of soils based on unconfined compressive strength test (基于无侧限抗压强度试验的土壤离散元参数标定). *Transactions of the Chinese Society of Agricultural Engineering*, vol.36, no.13, pp. 39-47. Beijing/China.

[24] Zhang T., Pang Y., Song S., Wu Y., Pan L., Shao W., Yang M., Tang X., Wang Y., Li X., (2021). Design of small potato combine harvester under heavy soil (黏重土壤下小型马铃薯联合收获机设计). *South China Agriculture*, vol. 15, no. 16, pp. 98-101+115. Chongqing/China.

[25] Zhongcai W., Hongwen L., Guangzhu S., Guoliang S., Wenzheng L., Xueqiang L., (2019). Experiments and analysis of a conveying device for soil separation and clod-crushing for a potato harvester. *Applied Engineering in Agriculture*, vol. 35, no.6. pp. 987-996. United States.

[26] Zhongcai W., Guoliang S., Xueqiang L., Faming W., Chuanzhu S., Pengxiang M., (2020)Parameter Optimization and Test of Potato Harvester Wavy Sieve Based on EDEM (基于离散元的马铃薯收获机波浪形筛面参数优化与试验). *Transactions of the Chinese Society of Agricultural Engineering*, vol.51, no.10, pp.35-42, Beijing/China.

[27] Zhou J., Yang S., Li M., Chen Z., Zhou J., Gao Z., Chen J., (2021). Design and experiment of a self-propelled crawler-potato harvester for hilly and mountainous areas. *INMATEH-Agricultural Engineering*, vol. 64, no. 2, pp. 1-8. Bucharest/Romania.